Hindawi
Science and Technology of Nuclear Installations
Volume 2022, Article ID 6319628, 13 pages
https://doi.org/10.1155/2022/6319628

Research Article

Control Rod Modeling and Worth Calculation for a Typical 1100 MWe Nuclear Power Plant Using WIMS/D4 and CITATION

Izza Shahid,[1] Nadeem Shaukat ,[2] Amjad Ali,[1] Meer Bacha,[1] Ammar Ahmad,[1] Muhammad Tariq Siddique,[3] Rustam Khan,[1] Sajjad Tahir,[1] and Zeeshan Jamil[4]

[1]*Department of Nuclear Engineering, Pakistan Institute of Engineering and Applied Sciences, P.O. Nilore 45650, Islamabad, Pakistan*
[2]*Center for Mathematical Sciences (CMS), Pakistan Institute of Engineering and Applied Sciences, P.O. Nilore 45650, Islamabad, Pakistan*
[3]*Department of Physics and Applied Mathematics (DPAM), Pakistan Institute of Engineering and Applied Sciences, P.O. Nilore 45650, Islamabad, Pakistan*
[4]*Key Laboratory of Neutronics and Radiation Safety, Institute of Nuclear Energy Safety Technology, Chinese Academy of Sciences, Beijing, China*

Correspondence should be addressed to Nadeem Shaukat; nadeem_shaukat07@hotmail.com

Received 3 May 2021; Revised 7 December 2021; Accepted 15 December 2021; Published 5 January 2022

Academic Editor: Arkady Serikov

A typical 1100 MWe pressurized water reactor (PWR) is a second unit installed at the coastal site of Pakistan. In this paper, verification analysis of reactivity control worth by means of rod cluster control assemblies (RCCAs) for startup and operational conditions of this typical nuclear power plant (CNPP) has been performed. Neutronics analysis of fresh core is carried out at beginning of life (BOL) to determine the effect of grey and black control rod clusters on the core reactivity for startup and operating conditions. The combination of WIMS/D4 and CITATION computer codes equipped with JENDL-3.3 data library is used for the first time for core physics calculations of neutronic safety parameters. The differential and integral worth of control banks is derived from the computed results. The effect of control bank clusters on core radial power distribution is studied precisely. Radial power distribution in the core is evaluated for numerous configurations of control banks fully inserted and withdrawn. The accuracy of computed results is validated against the reference values of Nuclear Design Report (NDR) of 1100 MWe typical CNPP. It has been observed that WIMS-D4/CITATION shows its capability to effectively calculate the reactor physics parameters.

1. Introduction

One of the most crucial tasks in controlling a nuclear reactor is to ensure its criticality. Neutron population must be increased slowly and in a very controlled manner when a nuclear reactor is starting up. There are three types of reactivity controls used in a nuclear reactor: burnable poison, chemical shim (boric acid), and moveable control rods. The moderator temperature coefficient decreases and becomes less negative with the increase of boric acid concentration. Since concentration of soluble boron significantly affects the moderator temperature coefficient at beginning of life, at very high concentration of boron, the positive moderator temperature coefficient at beginning of life is allowed to a certain limit. Therefore, the negative moderator temperature coefficient is ensured during power operational condition by reducing the soluble boron concentration and burnable poison rods used in the 1st cycle. In conventional pressurized water reactor (PWR) designs, soluble boron is used for reactivity control over core fuel cycle. Insertion of positive reactivity as a result of boron dilution accident due to sudden reduction of the boron concentration has a negative impact on PWR safety. Soluble boron corrosion presents a significant maintenance problem for pressurized water reactors, which use borated water to control reactivity during normal plant operations. Soluble boron can severely degrade low-alloy and carbon steel under the right conditions. Borated water leaks can lead to significant corrosion problems due to boric acid concentration as the water boils off or evaporates [1, 2]. Compact burnable BA materials have been used as an alternative to the traditional materials (i.e., B_4C and Ag-In-Cd). Different properties including higher density, good thermophysical properties, radiation resistance, and swelling resistance are possessed by these materials. Gadolinium, erbium, dysprosium, hafnium, and dysprosium as the most interesting rare earth nuclides for neutron absorption have already been studied in PWRs for cycle length extension. It has been observed that these suggested control rod materials achieve a satisfactory control rod worth (CRW) which is comparable with the CRW of the standard AIC control rods [3]. The effect of Europium and Pyrex on the neutronic characteristics of PWR has also been studied and compared with the traditional burnable absorbers (i.e., B_4C and Ag-In-Cd). The thermal neutron flux and the power distributions have been analyzed in PWR assembly to investigate the effect of Gadolinium and Europium on it. Through burnup calculations, ^{239}Pu and ^{241}Pu concentrations have been calculated for the suggested BAs materials [4].

Control rod reactivity worth calculation is pivotal for a nuclear reactor. Control rods are used for scramming of the reactor in case of an emergency [5–8]. After shutdown, the control rods provide the excess reactivity to the core during reactor startup in Xenon peaking. Control rod worth also depends upon location as neutron flux is a function of position in the core. Control rod worth is also a function of fuel and moderator temperature [8]. Control rod worth can be estimated using experimental procedures such as rod-drop method, positive period method, method of inverse kinetics, and periodic power modulation [9]. During the nuclear reactor design phase, we need software that can model a nuclear reactor core to its realistic conditions for analysis and benchmarking purposes. Control rod reactivity worth determines the reactivity swing when control rods move from full withdrawn to full insertion position. Reactivity worth of control rods can be assessed in two ways which are differential worth and integral worth. Integral worth is the total reactivity worth of the rod at that particular degree of withdrawal and is usually defined to be the greatest when the rod is fully withdrawn. Differential worth is the reactivity change per unit movement of the control rod and is expressed in units of reactivity per unit length. The reactivity worth is largest in the vicinity of maximum neutron flux which is usually at the center [10]. The rod cluster control assemblies (RCCAs) provide a mean of independent reactivity control system for the typical 1100 MWe CNPP. The RCCAs provide offset to compensate the reactivity effects arising from changes in fuel and moderator density and the accompanying power level change over the entire range from full load to no load. An important feature of this reactivity control system is the incorporation of black and grey control rods which provide better load follow capability [10–12].

Deterministic and stochastic methods can be used to estimate control rod worth. In deterministic methods, neutron transport equation is solved to generate macroscopic cross-sections for assemblies and diffusion equation is solved for the whole core calculations [7]. Batan-2diff which is a 2-dimensional diffusion theory code has been used for the modeling of the whole core. Axial buckling is provided while analyzing a 2D core [10]. The control rod reactivity worth of VVER-1000 reactor has been estimated in a PWR type reactor having 163 hexagonal fuel assemblies. Each fuel assembly includes 311 fuel rods, 18 guide channels, one central tube, and one tube for instrumentation. DRAGON4 has been used to simulate the fuel assemblies and reflector to compute group constants. In next step, these generated cross-sections are fed to DONJON4 to simulate the reactor core. DONJON4 solves the diffusion equation to simulate the core [12]. The results obtained by DRAGON4/DONJON4 were compared with those results obtained by Fadaei and Setayeshi [13] in their analysis of the same reactor using WIMS and CITATION. They explain that WIMS/D4 extracts the microscopic cross-sections from its library tape. Using this data, it calculates the macroscopic cross-sections for each material, incorporating the resonance shielding. The preliminary spectrum has been computed (many groups, few regions) using probability methods while for the neutron transport (many regions, condensed groups) either WDSN or collision probability can be employed [14–23]. The reactivity worth of two control rods of the GRR-1 reactor has been assessed using the deterministic code system NITAWL [24] and XSDRNPM [25], both modules of the SCALE system, and CITATION [26]. They used a Monte Carlo based code TRIPOLI [27–29] for stochastic approach.

WIMSD and CITATION have not been used previously for the domestic typical 1100 MWe CNPP for the analysis of reactivity control. In the present study, analysis of reactivity control by means of black and grey control rod clusters is presented for both the startup and operational conditions of this typical nuclear power plant. The objective of this work is to verify the reactivity effects of black and grey rods on core power distribution. In this perspective, control rods worth and associated reactivity effects upon power distribution have been analyzed for several core configurations at startup and operational conditions. A comparison of computed results with the reference values contained in Nuclear Design Report (NDR) is also presented.

2. Reactor Description

The reactor core of typical 1100 MWe CNPP consists of 177 fuel assemblies (FAs). Each assembly is composed of 17×17 rod array comprising 264 fuel rods, 24 guide tubes, and one instrumentation thimble. Fuel rods contain slightly enriched uranium dioxide pellets which are stacked in cold pressed Zr-4 tubes. Fuel assemblies are loaded with three different enrichments in the initial core; these are 1.8%, 2.4%, and 3.1%, respectively. The instrumentation thimble located at the center of assembly provides a channel for insertion of an in-core neutron detector. The guide tubes for control rods and the instrumentation tube are made of zircaloy. Basic information of core technical data is mentioned in Table 1. Two regions consisting of 2.4% and 1.8% enrichments are distributed to form a partial checkerboard pattern in the central portion of the core. The third region contains the highest enrichment and is arranged around the periphery of the core [30].

2.1. Fuel Enrichment and Loading. As mentioned earlier, fuel assemblies of the initial core are grouped according to three regions of enrichment, which are 1.8%, 2.4%, and 3.1% which consist of 61, 68, and 48 fuel assemblies, respectively. Fuel assemblies in the two low enrichment regions are mixed in the central region of the core in a checkerboard array. Fuel assemblies with highest enrichment are placed on the periphery of the core. Reactor core is designed with 12-month fuel management strategy with one-third of fuel assemblies to be discharged every year [30].

2.2. Rod Cluster Control Assemblies. There are 61 rod cluster control assemblies (RCCAs), out of which 49 are black and 12 grey clusters. The length of each control rod absorber is 4088.1 mm. The absorber material of black rods is Ag-In-Cd with weight composition: Ag 80%, In 15%, and Cd 5%. The grey rods are AISI 304 SS bars. The RCCAs are categorized into control rod banks and shutdown rod banks [30].

2.3. Control Rod Banks. Control rod banks are further categorized into two types: power compensation banks and temperature regulation banks. Power compensation banks (G1, G2, N1, and N2) are used to control core reactivity changes associated with step load changes and control power distribution. In Mode-G, grey rods (less absorbing control rods) are used to minimize perturbations of the core power distribution during rod insertion. With optimized overlapping, black and grey rods together provide full compensation for reactivity changes due to power level changes and reduce deformation in axial power distribution. Temperature regulation bank (R) controls core average temperature in order to maintain an accurate adjustment of reactivity by optimizing power axial distribution and residual reactivity changes [30].

2.4. Shutdown Rod Banks. Shutdown rod banks (SA, SB, and SC) are employed in case of reactor trip to shut down the reactor. Together with the control rod banks, shutdown rod banks drop into the core simultaneously to ensure negative reactivity required for shutdown [30].

2.5. Control Bank R and Its Insertion Limits. The control bank R provides fine adjustments of core reactivity independently. It has very high negative reactivity which allows it to provide temporary assistance to grey control banks during rapid power transients where reactivity insertion of the grey banks is limited by the maximum rate of control rod displacement [30].

2.6. Burnable Poison Assembly. A burnable poison assembly consists of burnable poison rods attached to a hold-down assembly. Burnable poison rods are made of borosilicate glass tubes (12.5% B_2O_3) which are contained in casing of stainless steel. The burnable poison rods provide partial control of excess reactivity available during the 1^{st} cycle. Burnable poison is used to accommodate excessive reactivity, reduce the boron concentration in the coolant in the first core, maintain the negative moderator temperature coefficient of reactivity, and obtain the uniform radial power distribution of the core. There are 1248 burnable poison rods in the initial core with specific arrangement shown in NDR [30].

2.7. Neutron Source Assembly. The purpose of the neutron source assembly is to provide a base neutron level to ensure that the neutron detectors are operational and responding to core multiplication neutrons. Both the primary and secondary neutron source rods are used in the initial core. The primary source rod contains Cf-252, which releases neutrons spontaneously during first fueling and start-ups. The secondary source rod contains a stable material (Sb-Be), which is activated by neutron bombardment during reactor operation [30].

Number densities in barn/cm for fuel assemblies and burnable poison assemblies are calculated. Fuel used in fresh core is UO_2 with a density of 10.257 g/cm^3 at HZP. Pressurized helium gas is used between the fuel rods and inner cladding. Zircaoly-4 with a density of 6.55 g/cm^3 is used for fuel rods cladding. For material information in WIMS/D4, we either can opt for direct number density input or can give weight percent composition. Therefore, weight percent composition was given as the input for cladding. The concentration of 1073 ppm of borated water is used as coolant and moderator.

The number density calculations of borosilicate glass as burnable poison using the information provided in Table 1 are performed. The mass fraction of B_2O_3 is 12.5% in the first cycle of fresh core. Stainless steel (AISI 304) is used for the cladding of burnable poison; density used for SS (AISI 304) is 8 g/cm^3. Material consisting of silver, cadmium, and indium is used in control rods with a density of 10.17 g/cm^3. Stainless steel (AISI 316L) is used for the cladding of control material; density used for SS (AISI 316) is 7.9 g/cm^3.

3. Modeling and Simulation

Two available numerical solution techniques offered by WIMS/D4 are Discrete-Ordinate S_N (DSN) and Collison Probability (PERSEUS). WIMS version using DSN method based on cylindrical/slab S_N is applicable for pin cell and clustered with smeared region, while PERSEUS method uses first flight collision probability applicable to all 4 spatial models. DSN method solves transport equation in one dimension (r) while discretizing the direction variable (Ω). PERSEUS uses collision probability methods to solve transport equation in one dimension r. Fuel assemblies of

Table 1: Reactor core description (cycle-1) [30].

Active core		Fuel assemblies	
Equivalent diameter, cm	322.8	Number	177
Core average active fuel height, first core, cm (cold dimensions)	365.76	Rod array	17 × 17
Height-to-diameter ratio	1.13	Rods per assembly	264
Total cross-section area, cm^2	81848	Rod pitch, cm	1.26
Fuel rods		Overall transverse dimensions, cm	21.4 × 21.4
Number	46728	Number of guide thimbles per assembly	24
Outside diameter, mm	9.5	Composition of guide thimbles	Zircaloy-4
Diametric gap, mm	0.17	Fuel pellets	
Clad thickness, mm	0.57	Material	UO_2
Clad material	Zircaloy-4	Density (percent of theoretical)	95
Absorber rod cluster control assemblies		Fuel enrichments w%	
Neutron absorber	Ag-In-Cd	Region 1	1.8
Composition, %	80, 15, 5	Region 2	2.4
Diameter, mm	8.661	Region 3	3.1
Length, mm	3607	Diameter, mm	8.192
Density, g/cm^3	10.17	Height, mm	13.46
Cladding material	AISI 316L	Burnable poison rods (first core)	
Clad thickness, mm	0.47	Number of assemblies with BP rods	80
Grey rod cluster control assemblies		Material	Borosilicate glass
Number of grey RCCAs	12	Outside tube, O. D, mm	9.675
Number of absorber rods per cluster	12	Outside tube, I. D, mm	8.738
Black rod cluster control assemblies		Poison O. D, mm	8.54
Number of black RCCAs	49	Poison I. D, mm	4.83
Number of absorber rods per cluster	24	Inner tube, O. D, mm	4.615
		Inner tube, I. D, mm	4.275

K-2 reactor core are modeled by WIMS/D4 code in DSN method and PERSEUS method [11, 13].

WIMS (Winfrith Improved Multigroup Scheme) is a general-purpose multigroup transport theory based deterministic code. The version used here was developed in 1980 [11]. Reactor lattices can be modeled in WIMS for calculation of neutronic fluxes and multiplication factors. Cylindrical and slab geometries are the two main lattice types that can be modeled using WIMS. For the setting of WIMS input, it requires the material and geometric information from the user and uses a microscopic cross-section data library for neutronics calculations to generate macroscopic cross-sections. WIMS solves neutron transport equation to generate macroscopic cross-sections which are used by CITATION to simulate the complete core.

CITATION is designed to solve problems using the finite-difference representation of neutron diffusion theory, treating up to three space dimensions with arbitrary group-to-group scattering. It has also been designed to attack problems which can be run in a reasonable amount of time. Storage of data is allocated dynamically to give the user flexibility in dimensioning. Typically, a finite-difference diffusion problem could have 200 depleting zones, 10,000 nuclide densities, and 30,000 space-energy point flux values [11, 13].

Reactor core is modeled in hot zero power (HZP) with fuel, clad, and moderator at 564 K. Control rod worth calculations are performed at critical boron concentration for comparison of results with those mentioned in typical 1100 MWe CNPP Nuclear Design Report (NDR). The boron concentration for all the control rod clusters out at the beginning of cycle 1 is considered to be 1073 ppm. In NDR calculation results, ELEMENT code uses microscopic data macroscopic constants for homogenized core regions, including group constants for control rods with self-shielding. COROCA code based on 2D 2-group diffusion evaluation theory is used for core calculations. In the present study, WIMS/D4 and CITATION codes are used for cross-section generation and core calculations.

Water reflector is considered around the core. Square PWR assemblies cannot be modeled in the used version of WIMS/D4; therefore, cylindrical rod cluster has been used conserving the rod pitch, assembly pitch, and assembly volume. Square lattice is modeled in the form of ring. Annular material region of each rod is specified together with its dimensions and position in (R, Θ) plane. Figure 1 represents the conversion of square geometry to cylindrical rod cluster [23].

For the determination of reactivity worth of control rods, macroscopic cross-sections are generated by WIMS/D4 and these cross-sections are given as input to CITATION which shall be used to model the full core. The procedure can be represented in the following way:

(1) Macroscopic cross-section data is generated using WIMS/D4 for each region like fuel, burnable poison, and cluster rod assemblies

(2) Using the cross-sections generated above, the whole core is modeled in CITATION providing geometrical information for generation of effective multiplication factor, neutronic fluxes, and average power densities

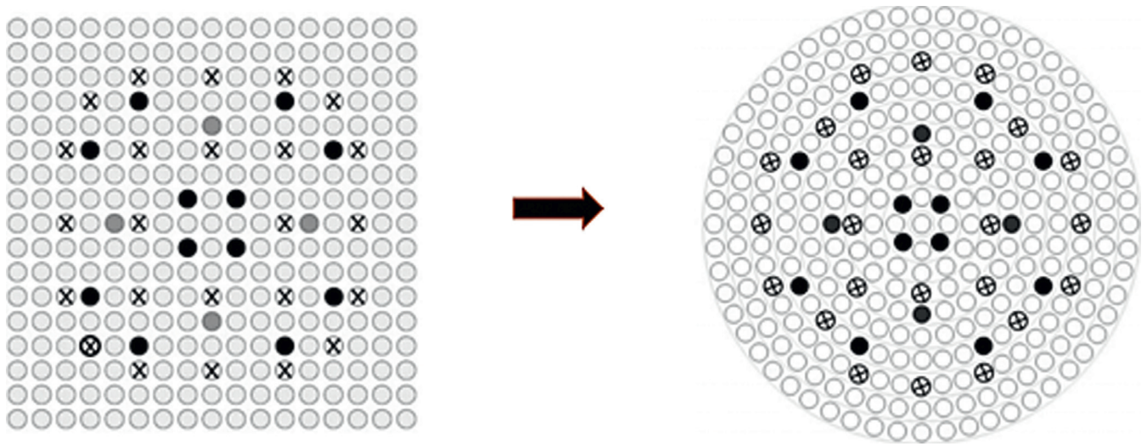

Figure 1: Conversion of square lattice assemblies into rod cluster assemblies.

Figure 2 shows the working scheme of WIMS/D4 and CITATION. JENDL-3.3 is used as WIMS/D4 microscopic cross-section library. The full core including 177 fuel assemblies is modeled in CITATION giving macroscopic cross-sections for each assembly. Suitable mesh spacing is selected. Most of the calculations are performed with 2D model of the core giving axial buckling in the input. Differential worth is calculated using 3D model of the core in CITATION. Water reflector is considered around the core.

4. Numerical Results and Discussion

Reactivity is calculated in pcm while the relative error (RE) in reactivity is calculated using the following formula:

$$\text{relative error [\%]} = \left|\frac{\text{calculated value} - \text{reference value}}{\text{reference value}}\right| \times 100. \quad (1)$$

A number of analyses have been carried out to calculate integral worth of all control banks for the critical core at startup conditions. The core power distribution has also been determined for some configurations of control rod banks at hot zero power (HZP). The control banks worth is calculated at beginning of cycle, hot zero power (HZP), and no xenon (NOXE) conditions for the critical core (with average critical boron concentration). These results have been compared with the reference data quoted in NDR for typical 1100 MWe CNPP.

The individual reactivity worth of control rod banks has been calculated using both DSN and PERSEUS sequence. The results are compared with the NDR values and shown in Table 2. The calculated bank worth for N1 and N2 using DSN sequence is 799 pcm and 1144 pcm, respectively, having the difference of less than 10% from the reference values, while using PERSEUS sequence, these are 4.75% and 1.66%, respectively, having a difference of less than 5% from the reference values as shown in Table 2. The control rod worth calculated from DSN sequence for SA, SB, SC, and *R* is 1040 pcm, 1266 pcm, 719 pcm, and 1201 pcm, respectively, which differ from reference data by 0.76%, 0.31%, 0.7%, and 2.12%, respectively. The control rod worth calculated from PERSEUS sequence for SA, SB, SC, and *R* is 995 pcm, 1233 pcm, 664 pcm, and 1158 pcm, respectively, which differ from reference data by 5.1%, 2.93%, 6.95%, and 5.7%, respectively. The calculated value of control rod worth of bank G1 using DSN sequence at BOL, HZP, and NOXE is 516 pcm and for control bank G2, the value is 991 pcm which differ from the reference value by 21.7% and 22.3%, respectively. The calculated value of control rod worth of bank G1 using PERSEUS sequence at BOL, HZP, and NOXE is 507 pcm and for control bank G2, and the calculated worth is 986 pcm which differ from the reference value by 16.1% and 17.7%, respectively. These differences are due to the homogenization effect of diffusion theory code. In actuality, there is more heterogeneity in these banks while the macroscopic cross-sections generated by WIMSD are homogenized.

Radial power distribution has been evaluated for the various configurations of rodded (control bank fully inserted) and unrodded (control bank fully withdrawn) core at BOL and NOXE conditions. The analysis for relative power distribution is performed for fresh core with reflector at HZP, ARO, and no xenon using PERSEUS sequence. The plot for the corresponding radial power distribution is shown in Figure 3(a). Relative power distributions for fresh core with reflector at HZP, no xenon with bank G1 inserted, with bank G1 and G2 inserted, with bank R1 inserted, with bank R1 and G1 inserted, with bank R1, G1 and G2 inserted and with Bank R1, G1, G2, and N1 inserted using PERSEUS sequence are shown in Figures 4(a) to 4(f), respectively. Grey control rod assemblies (G1 and G2) being heterogeneous assemblies produces a notable error. The reason for somewhat higher percentage error in radial power on the assemblies at the core periphery is homogenization theory. Simple flux-volume averaged cross-sections are used in transport/diffusion theory codes rather than discontinue factors of advanced equivalent homogenization theory. The flux near the reflectors show understandable slope and the diffusion theory becomes no more applicable in the vicinity of absorbing materials or reflectors. Moreover, the other possible reasons of these discrepancies may come from difference of library and computational model (energy groups homogenization and geometry approximations).

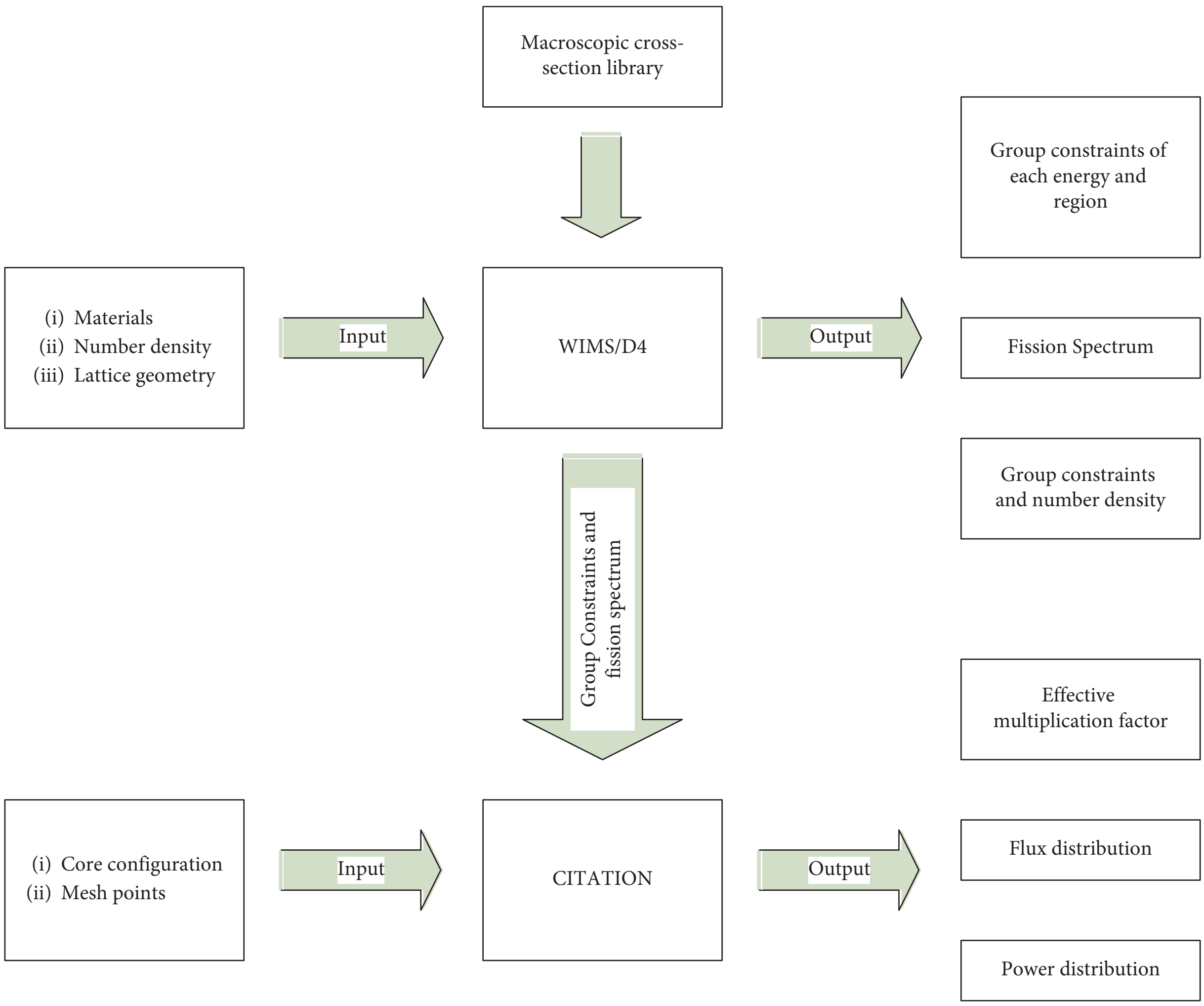

Figure 2: Calculation scheme for WIMSD and CITATION.

Table 2: Results for individual reactivity worth of control rod banks.

Rod banks inserted	NDR	Reactivity worth using DSN sequence (pcm)		Reactivity worth using PERSEUS sequence (pcm)	
		CITATION	Relative error (%)	CITATION	Relative error (%)
SA	1048	1040	0.76	995	5.1
R	1227	1201	2.12	1158	5.7
SB	1270	1266	0.31	1233	2.93
SC	714	719	0.7	664	6.95
N1	839	799	4.76	801	4.75
N2	1042	1144	9.78	983	1.66
G1	424	516	21.7	507	16.1
G2	810	991	22.3	986	17.7
Total worth	7374	7671	4.03	7281	0.09

The power distribution for fresh core with reflector at HZP, ARO, and no xenon using DSN sequence is shown in Figure 3(b). Relative power distributions for fresh core with reflector at HZP, no xenon with bank G1 inserted, with bank G1 and G2 inserted, with bank R1 inserted, with bank R1 and G1 inserted, with bank R1, G1 and G2 inserted and with Bank R1, G1, G2, and N1 inserted using DSN sequence are represented in Figures 5(a) to 5(f), respectively.

In the first case given below, differential and integral worth of bank G1 at BOL, HZP with no xenon is calculated. The results for differential and integral are shown in Figures 6(a) and 7(a), respectively. Differential and integral worth of bank G2 (G1 inserted), of bank N1 (G1 and G2 inserted), at BOL, HZP, and no xenon is calculated. The results for differential and integral are shown in Figures 6(b) and 7(b), respectively. Differential and integral worth of

	H	G	F	E	D	C	B	A
8	0.79 0.79 0.00	0.79 0.79 0.00	0.88 0.91 3.29	0.97 0.99 2.02	1.10 1.09 0.91	1.32 1.24 6.45	1.19 1.19 0.00	1.09 1.06 2.83
9	0.79 0.79 0.00	0.84 0.86 2.33	0.89 0.92 3.26	0.96 0.99 3.03	1.05 1.07 1.87	1.14 1.15 0.87	1.16 1.16 0.00	1.19 1.12 6.25
10	0.88 0.91 3.29	0.89 0.92 3.26	0.92 0.96 4.17	0.96 1.00 4.00	0.99 1.04 4.81	1.05 1.09 3.67	1.23 1.23 0.00	0.96 0.84 14.3
11	0.97 0.99 2.02	0.96 0.99 3.03	0.96 1.00 4.00	0.96 1.01 4.95	0.98 1.02 3.92	0.95 1.00 5.00	0.87 0.84 3.57	
12	1.10 1.09 0.91	1.06 1.07 0.93	1.00 1.04 3.85	0.98 1.02 3.92	0.95 1.01 5.94	0.98 1.00 2.00	0.71 0.64 10.9	
13	1.33 1.24 7.26	1.15 1.15 0.00	1.06 1.09 2.75	0.96 1.00 4.00	0.98 1.00 2.00	0.83 0.73 13.7		
14	1.19 1.19 0.00	1.16 1.16 0.00	1.24 1.23 0.81	0.87 0.84 3.57	0.72 0.64 12.5			
15	1.09 1.06 2.83	1.19 1.12 6.25	0.96 0.84 14.3					

Calculated
Reference
% Error

(a)

	H	G	F	E	D	C	B	A
8	0.76 0.79 3.79	0.75 0.79 5.06	0.85 0.91 6.59	0.91 0.99 8.09	1.03 1.09 5.50	1.17 1.24 5.56	1.19 1.19 0.00	1.13 1.06 6.6
9	0.75 0.79 5.06	0.81 0.86 5.82	0.85 0.92 7.61	0.93 0.99 6.06	1.00 1.07 6.54	1.12 1.15 2.61	1.16 1.16 0.00	1.28 1.12 14.3
10	0.85 0.91 6.59	0.85 0.92 7.61	0.89 0.96 7.30	0.92 1.00 8.00	0.99 1.04 4.81	1.05 1.09 3.67	1.32 1.23 7.32	1.05 0.84 25
11	0.91 0.99 8.08	0.93 0.99 6.06	0.92 1.00 8.00	0.95 1.01 5.94	0.97 1.02 4.90	0.98 1.00 2.00	0.90 0.84 7.14	
12	1.03 1.09 5.50	1.00 1.07 6.54	0.99 1.04 4.81	0.97 1.02 4.90	0.98 1.01 2.97	1.00 1.00 0.00	0.75 0.64 17.2	
13	1.17 1.24 5.64	1.12 1.15 2.61	1.06 1.09 2.75	0.99 1.00 1.00	1.00 1.00 0.00	0.87 0.73 19.2		
14	1.19 1.19 0.00	1.17 1.16 0.86	1.32 1.23 7.32	0.90 0.84 7.14	0.75 0.64 17.2			
15	1.13 1.06 6.60	1.28 1.12 14.3	1.06 0.84 26.1					

Calculated
Reference
% Error

(b)

Figure 3: Radial power distribution of cycle 1 at HZP, ARO, and no xenon (a) using PERSEUS sequence and (b) using DSN sequence.

	H	G	F	E	D	C	B	A
8	0.77 0.79 2.53	0.77 0.77 0.00	0.81 0.86 5.81	0.76 0.82 7.32	0.52 0.62 16.1	1.12 1.10 1.82	1.19 1.20 0.83	1.15 1.11 3.63
9	0.77 0.77 0.00	0.80 0.84 4.76	0.84 0.88 4.54	0.84 0.90 6.66	0.87 0.92 5.43	1.06 1.09 2.75	1.19 1.19 0.00	1.28 1.18 8.45
10	0.81 0.86 5.81	0.84 0.88 4.54	0.89 0.94 5.32	0.94 0.98 4.08	0.99 1.04 4.80	1.09 1.12 2.68	1.32 1.30 1.54	1.05 0.90 16.6
11	0.76 0.82 7.31	0.84 0.90 6.66	0.94 0.98 4.08	0.99 1.05 5.71	1.05 1.08 2.78	1.05 1.08 2.78	0.97 0.91 6.59	
12	0.53 0.62 14.5	0.87 0.92 5.43	0.99 1.04 4.81	1.05 1.08 2.78	1.07 1.11 3.60	1.12 1.11 0.90	0.82 0.71 15.5	
13	1.13 1.10 2.72	1.07 1.09 1.83	1.09 1.12 2.67	1.05 1.08 2.78	1.13 1.11 1.80	0.96 0.82 17.1		
14	1.20 1.20 0.00	1.20 1.19 0.84	1.33 1.30 2.31	0.97 0.91 6.59	0.82 0.71 15.5			
15	1.16 1.11 4.54	1.29 1.18 9.32	1.06 0.90 17.8					

Calculated
Reference
% Error

(a)

	H	G	F	E	D	C	B	A
8	0.79 0.86 8.14	0.78 0.83 6.02	0.78 0.88 11.3	0.70 0.80 12.5	0.50 0.60 16.7	1.22 1.18 3.39	1.43 1.40 2.14	1.44 1.33 8.27
9	0.78 0.83 6.02	0.80 0.88 9.09	0.79 0.88 10.2	0.72 0.83 13.3	0.73 0.82 10.9	1.10 1.12 1.78	1.40 1.36 2.94	1.59 1.40 13.5
10	0.78 0.88 11.3	0.79 0.88 10.2	0.77 0.88 12.5	0.71 0.82 13.4	0.49 0.61 19.6	1.03 1.06 2.83	1.50 1.43 4.89	1.26 1.04 21.2
11	0.71 0.80 11.3	0.72 0.83 13.3	0.71 0.82 13.4	0.78 0.88 11.4	0.87 0.94 7.44	1.03 1.06 2.83	1.06 0.97 9.28	
12	0.51 0.60 15.0	0.74 0.82 9.76	0.49 0.61 19.7	0.87 0.94 7.44	1.03 1.07 3.74	1.16 1.13 2.65	0.89 0.75 18.7	
13	1.24 1.18 5.08	1.11 1.12 0.89	1.03 1.06 2.83	1.03 1.06 2.83	1.16 1.13 2.65	1.03 0.85 21.2		
14	1.44 1.40 2.86	1.42 1.36 4.41	1.51 1.43 5.59	1.06 0.97 9.27	0.89 0.75 18.7			
15	1.46 1.33 9.77	1.61 1.40 15.0	1.28 1.04 23.1					

Calculated
Reference
% Error

(b)

Figure 4: Continued.

	H	G	F	E	D	C	B	A
8	0.73 0.74 1.35	0.72 0.72 0.00	0.79 0.83 4.82	0.93 0.96 3.13	1.05 1.07 1.87	1.09 1.03 5.83	0.54 0.50 08.0	0.76 0.71 7.04
9	0.72 0.72 0.00	0.72 0.74 2.7 0	0.73 0.75 2.67	0.89 0.94 5.32	1.06 1.08 1.85	1.07 1.09 1.83	0.96 0.95 1.05	1.00 0.91 9.89
10	0.8 0.83 3.61	0.73 0.75 2.67	0.42 0.44 4.54	0.87 0.91 4.39	1.08 1.15 6.09	1.16 1.21 4.13	1.29 1.29 0.00	0.96 0.82 17.1
11	0.94 0.96 2.08	0.89 0.94 5.32	0.88 0.91 3.29	1.02 1.09 6.42	1.17 1.24 5.65	1.18 1.26 6.35	1.05 1.02 2.94	
12	1.06 1.07 0.93	1.06 1.08 1.85	1.09 1.15 5.22	1.17 1.24 5.65	1.24 1.33 6.76	1.32 1.35 2.2 2	0.95 0.85 11.7	
13	1.11 1.03 7.77	1.08 1.09 0.92	1.17 1.21 3.31	1.19 1.26 5.55	1.32 1.35 2.22	1.15 1.02 12.7		
14	0.54 0.50 8.00	0.97 0.95 2.11	1.3 1.29 0.78	1.06 1.02 3.92	0.96 0.85 12.9			
15	0.77 0.71 8.45	1.01 0.91 10.9	0.97 0.82 18.3					

Calculated
Reference
% Error

(c)

	H	G	F	E	D	C	B	A
8	0.69 0.70 4.28	0.66 0.67 1.49	0.65 0.75 8.00	0.69 0.76 9.21	0.49 0.58 15.5	0.88 0.87 1.15	0.54 0.48 12.5	0.82 0.73 12.3
9	0.66 0.67 1.49	0.66 0.69 4.34	0.65 0.68 4.41	0.75 0.82 8.53	0.85 0.92 7.61	0.98 1.02 3.92	0.99 0.96 3.13	1.09 0.95 14.7
10	0.70 0.75 6.66	0.66 0.68 2.94	0.43 0.42 2.38	0.85 0.90 5.55	1.07 1.16 7.75	1.20 1.24 3.22	1.39 1.36 2.2	1.05 0.88 19.32
11	0.70 0.76 7.89	0.76 0.82 7.31	0.85 0.90 5.55	1.06 1.15 7.83	1.26 1.34 5.97	1.30 1.38 5.97	1.16 1.11 4.50	
12	0.49 0.58 15.5	0.86 0.92 6.52	1.07 1.16 7.75	1.26 1.34 5.97	1.38 1.48 6.76	1.49 1.51 1.32	1.08 0.95 13.7	
13	0.90 0.87 3.45	0.99 1.02 2.94	1.20 1.24 3.22	1.30 1.38 5.79	1.49 1.51 1.32	1.32 1.15 14.78		
14	0.55 0.48 14.5	1.00 0.96 4.00	1.4 1.36 2.94	1.17 1.11 5.41	1.09 0.95 14.7			
15	0.83 0.73 19.0	1.10 0.95 15.8	1.05 0.88 19.32					

Calculated
Reference
% Error

(d)

	H	G	F	E	D	C	B	A
8	0.70 0.78 10.3	0.67 0.73 8.22	0.67 0.77 12.9	0.62 0.73 15.1	0.44 0.55 20.0	0.90 0.88 2.27	0.59 0.54 9.26	0.99 0.86 15.1
9	0.68 0.73 6.85	0.66 0.74 10.8	0.61 0.68 10.3	0.63 0.74 14.8	0.63 0.78 19.2	0.97 1.01 3.96	1.13 1.07 5.61	1.32 1.11 18.9
10	0.68 0.77 11.6	0.61 0.68 10.3	0.37 0.38 2.63	0.63 0.72 12.5	0.53 0.67 20.9	1.12 1.18 5.08	1.56 1.50 4.00	1.25 1.01 23.7
11	0.63 0.73 13.7	0.63 0.74 14.9	0.63 0.72 12.5	0.86 0.99 13.1	1.11 1.22 9.02	1.33 1.41 5.67	1.30 1.22 6.55	
12	0.45 0.55 18.2	0.68 0.78 12.82	0.54 0.67 19.4	1.10 1.22 9.84	1.43 1.53 6.57	1.65 1.64 0.61	1.24 1.06 16.9	
13	0.93 0.88 5.68	0.98 1.01 2.97	1.13 1.18 4.23	1.33 1.41 5.67	1.65 1.64 0.61	1.51 1.28 17.9		
14	0.64 0.54 18.5	1.14 1.07 6.54	1.58 1.50 5.33	1.34 1.22 9.83	1.25 1.06 17.9			
15	1.03 0.86 19.7	1.35 1.11 21.6	1.27 1.01 25.7					

Calculated
Reference
% Error

(e)

	H	G	F	E	D	C	B	A
8	0.36 0.39 7.69	0.33 0.35 5.71	0.23 0.24 4.17	0.47 0.57 17.5	0.49 0.62 20.9	1.16 1.18 1.69	0.86 0.78 10.3	1.44 1.30 10.8
9	0.33 0.35 5.72	0.35 0.38 7.89	0.36 0.41 12.2	0.51 0.63 19.0	0.74 0.88 15.9	1.21 1.32 8.33	1.51 1.50 0.66	1.86 1.64 13.4
10	0.23 0.24 4.17	0.37 0.41 9.76	0.28 0.29 3.45	0.53 0.63 15.8	0.52 0.67 22.4	1.27 1.38 7.97	1.95 1.96 0.51	1.68 1.42 18.3
11	0.48 0.57 15.8	0.53 0.63 15.8	0.54 0.63 14.3	0.67 0.78 14.1	0.82 0.9 8.88	1.23 1.31 6.11	1.41 1.32 6.81	
12	0.50 0.62 19.4	0.75 0.88 14.7	0.53 0.67 20.9	0.82 0.90 8.89	0.61 0.57 7.01	1.23 1.17 5.13	1.13 0.95 18.9	
13	1.19 1.18 0.85	1.24 1.32 6.06	1.29 1.38 6.52	1.24 1.31 5.34	1.24 1.17 5.98	1.15 0.91 26.4		
14	0.88 0.78 12.82	1.56 1.50 4.0	1.99 1.96 1.53	1.43 1.32 8.33	1.14 0.95 20.0			
15	1.48 1.30 13.8	1.89 1.64 15.2	1.71 1.42 20.4					

Calculated
Reference
% Error

(f)

FIGURE 4: Radial power distribution of cycle 1 using PERSEUS sequence at HZP, no xenon with (a) bank G1 inserted, (b) bank G1 and G2 inserted, (c) bank R1 inserted, (d) bank R1 and G1 inserted, (e) bank R1, G1, and G2 inserted, and (f) bank R1, G1, G2, and N1 inserted.

bank N1 (G1 and G2 inserted), of bank N2 (G1, G2 and N1 inserted), of bank R1 (G1, G2, N1 and N2 inserted) at BOL, HZP, and no xenon is calculated. The results for differential and integral worth are shown in Figures 6(c), 6(d), 7(c), and 7(d), respectively. With the insertion of control rod banks, more heterogeneity is being added in the system while cross-sections used are homogenized. This additional heterogeneity will add further error in the system. This error can be reduced by using some advanced codes having better capability of handling heterogeneity.

	H	G	F	E	D	C	B	A
8	0.72 0.79 8.86	0.71 0.77 7.79	0.76 0.86 11.6	0.71 0.82 13.4	0.49 0.62 20.4	1.00 1.10 9.09	1.21 1.20 0.83	1.20 1.11 8.11
9	0.71 0.77 7.79	0.76 0.84 9.53	0.78 0.88 11.4	0.80 0.90 11.1	0.82 0.92 10.87	1.05 1.09 3.67	1.21 1.19 1.68	1.38 1.18 16.95
10	0.77 0.86 10.5	0.78 0.88 11.4	0.85 0.94 9.57	0.89 0.98 9.18	0.98 1.04 5.77	1.09 1.12 2.67	1.41 1.30 8.46	1.15 0.90 27.7
11	0.71 0.82 13.4	0.80 0.90 11.1	0.89 0.98 9.18	0.98 1.05 6.67	1.03 1.08 4.63	1.08 1.08 0.00	0.99 0.91 8.79	
12	0.49 0.62 20.9	0.82 0.92 10.9	0.98 1.04 5.77	1.03 1.08 4.63	1.09 1.11 1.80	1.13 1.11 1.80	0.86 0.71 21.1	
13	1.00 1.10 9.09	1.05 1.09 3.67	1.09 1.12 2.68	1.08 1.08 0.00	1.13 1.11 1.80	1.00 0.82 21.9		
14	1.21 1.20 0.83	1.21 1.19 1.68	1.42 1.30 9.23	0.99 0.91 8.79	0.86 0.71 21.1			
15	1.21 1.11 9.01	1.39 1.18 17.8	1.15 0.90 27.8					

Calculated
Reference
% Error

(a)

	H	G	F	E	D	C	B	A
8	0.72 0.86 16.3	0.69 0.83 16.9	0.71 0.88 19.3	0.63 0.80 21.2	0.47 0.60 21.6	1.10 1.18 6.78	1.46 1.40 4.28	1.52 1.33 14.3
9	0.69 0.83 16.9	0.73 0.88 17.1	0.71 0.88 19.3	0.67 0.83 19.3	0.68 0.82 17.1	1.09 1.12 2.68	1.43 1.36 5.15	1.73 1.40 23.6
10	0.72 0.88 18.2	0.71 0.88 19.3	0.72 0.88 18.2	0.66 0.82 19.5	0.48 0.61 21.3	1.03 1.06 2.83	1.62 1.43 13.3	1.41 1.04 35.6
11	0.63 0.80 21.3	0.67 0.83 19.3	0.66 0.82 19.5	0.76 0.88 13.6	0.85 0.94 9.57	1.06 1.06 0.00	1.09 0.97 12.4	
12	0.47 0.60 21.7	0.68 0.82 17.1	0.48 0.61 21.3	0.85 0.94 -9.57	1.05 1.07 1.87	1.17 1.13 3.54	0.93 0.75 24.0	
13	1.10 1.18 6.78	1.09 1.12 2.68	1.03 1.06 2.83	1.06 1.06 0.00	1.18 1.13 4.42	1.07 0.85 25.9		
14	1.46 1.40 4.29	1.44 1.36 5.88	1.63 1.43 13.9	1.10 0.97 13.4	0.93 0.75 24.0			
15	1.52 1.33 14.3	1.74 1.40 24.3	1.41 1.04 35.6					

Calculated
Reference
% Error

(b)

	H	G	F	E	D	C	B	A
8	0.69 0.74 6.76	0.67 0.72 6.94	0.76 0.83 8.43	0.87 0.96 9.38	0.99 1.07 7.48	0.97 1.03 5.83	0.53 0.50 6.00	0.80 0.71 12.7
9	0.67 0.72 6.94	0.68 0.74 8.11	0.68 0.75 9.33	0.86 0.94 8.51	1.00 1.08 7.41	1.05 1.09 3.67	0.97 0.95 2.11	1.10 0.91 20.9
10	0.76 0.83 8.43	0.68 0.75 9.33	0.43 0.44 2.27	0.84 0.91 7.69	1.07 1.15 6.96	1.16 1.21 4.13	1.39 1.29 7.75	1.06 0.82 29.3
11	0.87 0.96 9.38	0.86 0.94 8.51	0.84 0.91 7.69	1.01 1.09 7.34	1.16 1.24 6.45	1.22 1.26 3.17	1.08 1.02 5.88	
12	1.00 1.07 6.54	1.00 1.08 7.41	1.07 1.15 6.96	1.16 1.24 6.45	1.27 1.33 4.51	1.34 1.35 0.74	1.00 0.85 17.6	
13	0.97 1.03 5.83	1.05 1.09 3.67	1.16 1.21 4.13	1.22 1.26 3.17	1.34 1.35 0.74	1.20 1.02 17.7		
14	0.53 0.50 6.00	0.97 0.95 2.11	1.39 1.29 7.75	1.08 1.02 5.88	1.00 0.85 17.7			
15	0.80 0.71 12.7	1.10 0.91 20.9	1.07 0.82 30.5					

Calculated
Reference
% Error

(c)

	H	G	F	E	D	C	B	A
8	0.62 0.70 11.4	0.59 0.67 11.9	0.64 0.75 14.7	0.64 0.76 15.8	0.46 0.58 20.7	0.78 0.87 10.3	0.53 0.48 10.4	0.85 0.73 16.4
9	0.59 0.67 11.94	0.61 0.69 11.59	0.59 0.68 13.24	0.71 0.82 13.41	0.80 0.92 13.04	0.97 1.02 4.90	1.00 0.96 4.17	1.18 0.95 24.2
10	0.65 0.75 13.3	0.59 0.68 13.2	0.40 0.42 4.76	0.80 0.90 11.1	1.06 1.16 8.62	1.20 1.24 3.23	1.49 1.36 9.56	1.16 0.88 31.8
11	0.64 0.76 15.8	0.71 0.82 13.4	0.80 0.90 11.1	1.05 1.15 8.70	1.24 1.34 7.46	1.34 1.38 2.90	1.20 1.11 8.11	
12	0.46 0.58 20.7	0.80 0.92 13.0	1.06 1.16 8.62	1.24 1.34 7.46	1.42 1.48 4.05	1.52 1.51 0.66	1.14 0.95 20.0	
13	0.78 0.87 10.3	0.97 1.02 4.90	1.20 1.24 3.23	1.34 1.38 2.90	1.52 1.51 0.66	1.38 1.15 20.0		
14	0.53 0.48 10.4	1.00 0.96 4.17	1.49 1.36 9.56	1.20 1.11 8.11	1.14 0.95 20.0			
15	0.85 0.73 16.4	1.18 0.95 24.2	1.16 0.88 31.8					

Calculated
Reference
% Error

(d)

	H	G	F	E	D	C	B	A
8	0.61 0.78 21.8	0.58 0.73 20.6	0.60 0.77 22.1	0.55 0.73 24.6	0.41 0.55 25.5	0.80 0.88 9.10	0.61 0.54 12.9	1.05 0.86 22.1
9	0.58 0.73 20.6	0.58 0.74 21.6	0.53 0.68 22.1	0.57 0.74 22.9	0.63 0.78 19.2	0.95 1.01 5.94	1.15 1.07 7.48	1.45 1.11 30.6
10	0.60 0.77 22.1	0.53 0.68 22.1	0.33 0.38 13.2	0.58 0.72 19.4	0.52 0.67 22.4	1.12 1.18 5.08	1.69 1.50 12.7	1.40 1.01 38.6
11	0.55 0.73 24.6	0.58 0.74 21.6	0.58 0.72 19.4	0.85 0.99 14.1	1.09 1.22 10.6	1.37 1.41 2.84	1.35 1.22 10.7	
12	0.41 0.55 25.5	0.63 0.78 19.2	0.52 0.67 22.4	1.09 1.22 10.7	1.46 1.53 4.58	1.68 1.64 2.44	1.31 1.06 23.6	
13	0.80 0.88 9.09	0.95 1.01 5.94	1.13 1.18 4.24	1.38 1.41 2.13	1.68 1.64 2.44	1.58 1.28 23.4		
14	0.61 0.54 12.9	1.15 1.07 7.48	1.69 1.50 12.7	1.35 1.22 10.7	1.31 1.06 23.6			
15	1.06 0.86 23.2	1.45 1.11 30.6	1.40 1.01 38.6					

Calculated
Reference
% Error

(e)

	H	G	F	E	D	C	B	A
8	0.30 0.39 23.1	0.26 0.35 25.7	0.19 0.24 20.8	0.41 0.57 28.1	0.45 0.62 27.4	1.02 1.18 13.6	0.84 0.78 7.69	1.50 1.30 15.4
9	0.27 0.35 22.8	0.29 0.38 23.7	0.31 0.41 24.4	0.47 0.63 25.4	0.68 0.88 22.7	1.19 1.32 9.85	1.54 1.50 2.67	2.03 1.64 23.7
10	0.20 0.24 16.7	0.31 0.41 24.4	0.24 0.29 17.2	0.48 0.63 23.8	0.50 0.67 25.8	1.27 1.38 -7.97	2.12 1.96 8.2	1.88 1.42 32.4
11	0.42 0.57 26.3	0.47 0.63 25.4	0.48 0.63 23.8	0.63 0.78 19.2	0.78 0.90 13.3	1.25 1.31 4.58	1.45 1.32 9.58	
12	0.45 0.62 27.4	0.69 0.88 21.6	0.51 0.67 23.9	0.78 0.90 13.3	0.58 0.57 1.75	1.22 1.17 4.27	1.18 0.95 24.2	
13	1.03 1.18 12.7	1.20 1.32 9.09	1.28 1.38 7.25	1.26 1.31 3.82	1.23 1.17 5.13	1.17 0.91 28.6		
14	0.85 0.78 8.97	1.56 1.50 4.00	2.14 1.96 9.18	1.47 1.32 11.4	1.18 0.95 24.2			
15	1.52 1.30 16.9	2.02 1.64 23.2	1.90 1.42 33.8					

Calculated
Reference
% Error

(f)

FIGURE 5: Radial power distribution of cycle 1 using DSN sequence at HZP, no xenon with (a) bank G1 inserted, (b) bank G1 and G2 inserted, (c) bank R1 inserted, (d) bank R1 and G1 inserted, (e) bank R1, G1, and G2 inserted, and (f) bank R1, G1, G2, and N1 inserted.

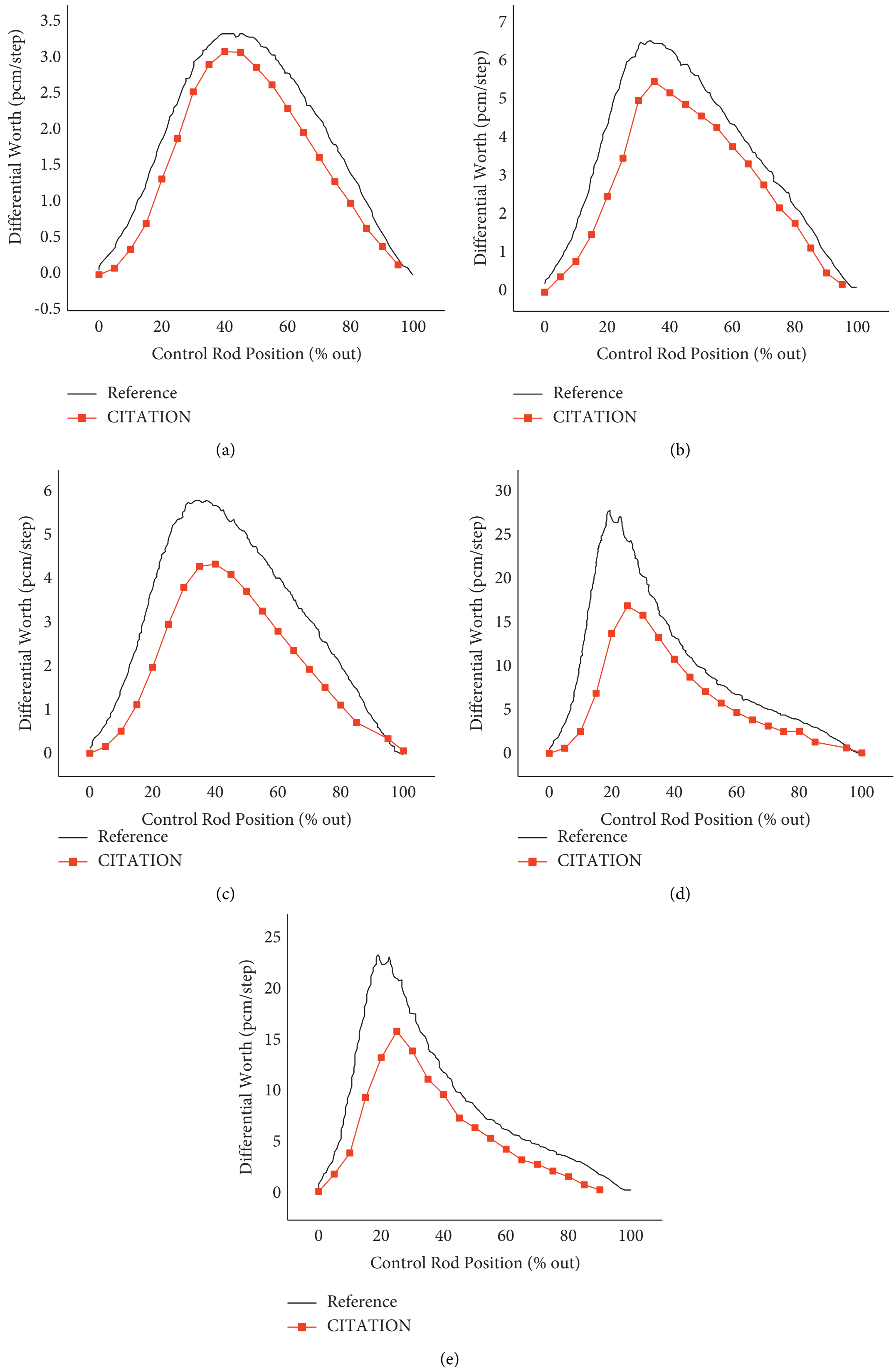

FIGURE 6: Differential rod worth at HZP, BOL, no xenon of (a) bank G1, (b) bank G2 (G1 inserted), (c) bank N1 (G1 and G2 inserted), (d) bank N2 (G1, G2, and N1 inserted), and (e) bank R1 (G1, G2, N1, and N2 inserted).

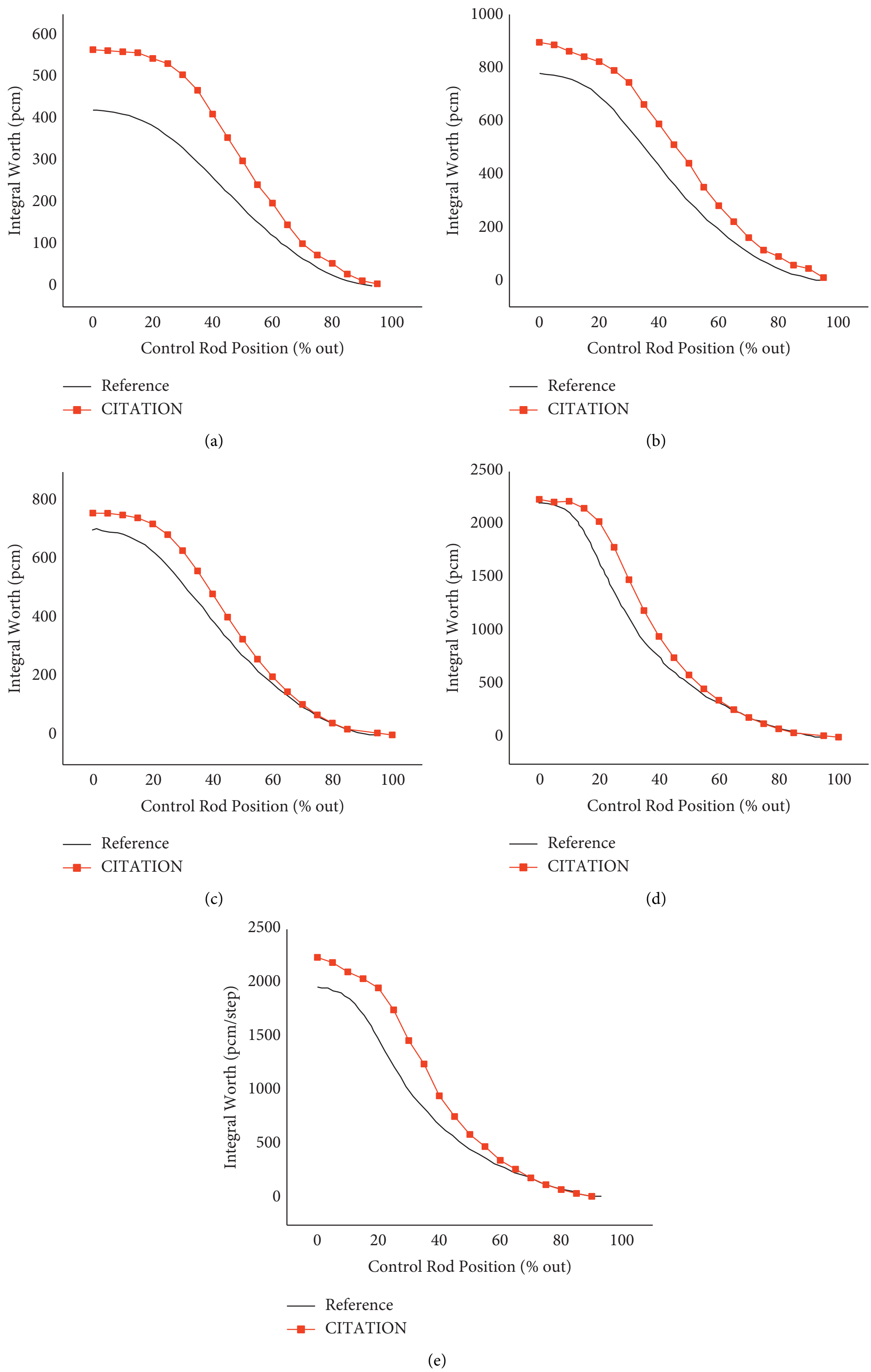

Figure 7: Integral rod worth at HZP, BOL, no xenon of (a) bank G1, (b) bank G2 (G1 inserted), (c) bank N1 (G1 and G2 inserted), (d) bank N2 (G1, G2, and N1 inserted), and (e) bank R1 (G1, G2, N1, and N2 inserted).

5. Conclusions

In the present work, a software package based on computer codes WIMS/D4 and CITATION equipped with JENDL-3.3 cross-section data library has been applied for the modeling of control rod and for calculation of the reactivity worth of the grey and black control rod clusters of a typical 1100 MWe CNPP. The individual control banks worth has been determined by analyzing its effect on reactivity for different configurations of rodded and unrodded cores. The consequent variations in radial power distribution have also been evaluated precisely. The differential and integral worth of control banks is derived from the computed results. The results are compared with the reference values cited in NDR of the nuclear power plant. The computed values of control rod banks worth are found to be in good agreement with the NDR values. Maximum deviation of 4.03% in combined integral control rod worth of the reactor with DSN sequence and 0.09% error with PERSEUS sequence is observed when compared with reference results. Due to addition of more heterogeneity in the system with the insertion of control rod banks, a notable error is added in the system. This error can be reduced by using some advanced codes having better capability of handling heterogeneity. The radial power distributions for different configurations of rodded and unrodded cores are also found in reasonable agreement with the design values, while the differences are large as compared to reference values reported in NDR. Grey control rod assemblies (G1 and G2) being heterogeneous assemblies produces a notable error due to the use of simple flux-volume averaged cross-sections rather than discontinue factors of advanced equivalent homogenization theory. It can be concluded that the latest tools can be used for the computation of neutronic safety parameters of nuclear reactor in various scenarios with acceptable accuracy, while WIMS/D4 and CITATION can also be used to achieve reasonable accuracy.

Data Availability

The data used to support the findings of this study are restricted by the Nuclear Agency of Pakistan. Data are available from the researchers who meet the criteria for access to confidential data.

Conflicts of Interest

The authors declare no conflicts of interest.

Acknowledgments

The authors sincerely appreciate funding from the research contract between Key Lab of Neutronics and Radiation Safety, INEST, CAS, China, and PIEAS, Pakistan.

References

[1] H. W. Graves, *Nuclear Fuel Management*, Wiley, Hoboken, NJ, USA, 1979.

[2] T. Jevremovic, *Nuclear Principles in Engineering*, Springer, Berlin, Germany, 2010.

[3] A. A. Galahom, "Investigation of different burnable absorbers effects on the neutronic characteristics of PWR assembly," *Annals of Nuclear Energy*, vol. 94, pp. 22–31, 2016.

[4] A. A. Galahom, "Study of the possibility of using Europium and pyrex alloy as burnable absorber in PWR," *Annals of Nuclear Energy*, vol. 110, pp. 1127–1133, 2017.

[5] M. Rahgoshay and O. Noori-Kalkhoran, "Calculation of control rod worth and temperature reactivity coefficient of fuel and coolant with burn-up changes for VVRS-2MWth nuclear reactor," *Nuclear Engineering and Design*, vol. 256, pp. 322–331, 2013.

[6] J. J. Duderstadt and L. J. Hamilton, *Nuclear Reactor Analysis*, Wiley, Hoboken, NJ, USA, 1976.

[7] Technical University Dresden, *Reactor Training Course Experiment: Control Rod Calibration*, Technical University Dresden, Institute of Power Engineering Training Reactor, Dresden, Germany, 2015.

[8] A. P. Meshik, *The Workings of an Ancient Nuclear Reactor*, Scientific American, NewYork, NY, USA, 2009.

[9] V. L. Putman, "Criticality safety basics, a study guide," Report, University of North Texas, Denton, TX, USA, 1999.

[10] T. M. Sembiring and L. P. Hong, "Validation of BATAN's standard diffusion codes on IAEA benchmark static calculation," *Atom Indonesia*, vol. 23, no. 2, pp. 73–91, 1997.

[11] M. N. Sarsam and B. M. Saied, "Neutronic flux and power distribution in a nuclear power reactor using WIMS-D4 and CITATION codes," *International Journal of Physics and Research*, vol. 2, pp. 23–29, 2012.

[12] F. Saadatian-Derakhshandeh, O. Safarzadeh, and A. S. Shirani, "Estimation of control rod worth in a VVER-1000 reactor using DRAGON4 and DONJON4," *Nukleonika*, vol. 59, no. 2, pp. 67–72, 2014.

[13] A. H. Fadaei and S. Setayeshi, "Control rod worth calculation for VVER-1000 nuclear reactor using WIMS and CITATION code," *Progress in Nuclear Energy*, vol. 51, no. 1, pp. 184–191, 2009.

[14] R. M. Westfall, L. M Petrie, N. M Greene, and J. l. Lucius, *NITAWL-S: Scale System Module for Performing Resonance Shielding and Working Library Production (NUREG/CR-0200-Vol2)*, U.S. Nuclear Regulatory Commission, Rockville, MD, USA, 2000.

[15] N. M. Greene and L. M. Petrie, *XSDRNPM-S: A One-Dimensional Discrete-Ordinates Code for Transport Analysis (NUREG/CR-0200-Vol2)*, RN:17040287, USA, 1984, https://inis.iaea.org/search/citationdownload.aspx.

[16] T. Fowler and D. Vondy, *Nuclear Reactor Core Analysis Code: CITATION*, Oak Ridge National Laboratory, Oak Ridge, TN, USA, 1969.

[17] S. Máté, "Assessing and enhancing nuclear safety and security culture for small facilities that handle radioactive material," *International Journal of Nuclear Security*, vol. 3, no. 1, pp. 12–15, 2017.

[18] J. R. Lamarsh and A. J. Baratta, *Introduction to Nuclear Engineering*, Prentice Hall, Inc., Hoboken, NJ, USA, 3rd edition, 2001.

[19] M. J. Halsall, *A Summary of WIMSD4 Input Options*, UKAEA, Abingdon, UK, 1980.

[20] T. Kulikowska, *Reactor Lattice Codes*, Institute of Atomic Energy, Otwock-Świerk, Poland, 2000.

[21] US Department of Energy, *DOE Fundamentals Handbook: Nuclear Physics and Reactor Theory*, US Department of Energy, Washington, DC, USA, 1993.

[22] International Atomic Energy Agency, *Research Reactor Core Conversion Guidebook*, IAEA, Vienna, Austria, 1992.

[23] T. Kulikowska, A. Stadnik, K. Andrzejewski, A. Beottcher, and M. Luszcz, "Application of the generally available WIMS versions to modern PWR," *Nukleonika*, vol. 57, no. 1, pp. 87–93, 2012.

[24] J. Ma, G. Wang, S. Yuan, H. Huang, and D. Qian, "An improved assembly homogenization approach for plate-type research reactor," *Annals of Nuclear Energy*, vol. 85, pp. 1003–1013, 2015.

[25] G. Girardin, G. Rimpault, P. Coddington, and R. Chawla, "Control rod shadowing and anti-shadowing effects in a large gas-cooled fast reactor," *Proceedings of ICAPP*, vol. 3, 2007.

[26] F. Arshad, S.-U.-I. Ahmad, and I. Haq, "PWR experimental benchmark analysis using WIMSD and PRIDE codes," *Annals of Nuclear Energy*, vol. 72, pp. 11–19, 2014.

[27] O. Petit, F. X. Hugot, Y. K. Lee, C. Jouanne, and A. Mazzolo, *TRIPOLI-4 Version 4 User Guide*, French Alternative Energies and Atomic Energy Commission, Paris, France, 2008.

[28] S. Kalcheva and E. Koonen, "Improved monte carlo-perturbation method for estimation of control rod worths in a research reactor," *Annals of Nuclear Energy*, vol. 36, no. 3, pp. 344–349, 2009.

[29] H. Oktajianto, E. Setiawati, K. Anam, and H. Sugito, "Analysis of high temperature reactor control rod worth for the initial and full core," *Journal of Physics: Conference Series*, vol. 799, Article ID 012017, 2017.

[30] Nuclear Power Institute of China, *1100 MWe typical nuclear design report*, Revision A, Report ID: 07S12-10YBG, Nuclear Power Institute of China, Beijing, China, 2014.